Technique for Determining Local Heat-Transfer Coefficients

H. J. Sternfeld* and J. Reinkenhof*
DFVLR, Lampoldshausen, Germany

This paper presents a procedure for determining the unsteady-state heat-transfer coefficient between a hot gas and a thermally thick wall with an arbitrary initial temperature distribution. The one-dimensional analysis takes into account the temperature dependence of the material properties and is based on the integral form of the energy conservation law. The measured unsteady temperature field is approximated by polynomials and power functions in space and time. Finally, the procedure for determining the heat-transfer coefficient is demonstrated for data obtained from an experimental fluorine/hydrogen rocket engine.

Nomenclature

A,B,C	= abbreviated terms
a,F,D	= coefficients
A, A_0	= areas
A_c	= cross-sectional area of the combustion chamber
A_t	= cross-sectional area of the nozzle throat
a_{ij}, a_k	= polynomial coefficients
α	= heat-transfer coefficient
b,d,G,E	= exponents
b	= polynomial coefficient
c	= specific heat
c,d	= polynomial coefficients
ϵ	= geometric parameter
L	= length
K	= thermal diffusivity
λ	= thermal conductivity
$\dot{m}_0$	= oxidizer mass-flow rate
$\dot{m}_F$	= fuel mass-flow rate
m	= summation index
n	= index
p_c	= combustion chamber pressure
q	= heat flux
ρ	= density
T	= temperature
T_w	= wall surface temperature
T_δ	= fluid temperature
t	= time
x	= coordinate of location
x_0, x_l	= control-volume boundaries
η_{c^*}	= characteristic velocity efficiency

Introduction

WHEN heat-transfer rates are calculated, dimensionless equations based on the theory of similitude require an experimental determination of local heat-transfer coefficients. If the heat flow from the moving fluid to the wall is steady, the heat-transfer coefficient can be derived from a local heat balance of the coolant.

If the wall features capacitive cooling, the heat flow is unsteady. A test arrangement working on this principle is simple and, if the heat flux is sufficiently large, it permits short testing periods. It only requires measurement of the unsteady temperature field in a wall serving as a heat sink. In this way, for example, local heat-transfer coefficients in rocket engines can be determined.[1-4]

The real difficulty in the experimental determination of the heat-transfer coefficient is not the measurement itself but evaluation of the data. Depending on the method of calculation, the local heat flux may yield widely different results.[5] If the temperatures in the heat conductor differ greatly, the temperature dependence of the material properties has to be taken into account. Then Fourier's differential equation of heat conduction becomes nonlinear, and the solutions indicated in Refs. 6 and 7 fail. Reference 8 describes a simple calculation method that permits the discrete determination of the heat flux $q=q(t)$ and heat-transfer coefficient $\alpha=\alpha(t)$ when the temperature $T=T(t)$ at a measurement point is known. This calls for a multiple solution of a system of linear equations which result from a heat balance of a number of finite elements of the heat conductor. This calculation is based on a known temperature distribution at time $t=0$, and when there is only a single temperature-measurement point, this method is limited to cases having a uniform initial-temperature distribution.

This paper presents a procedure for determining unsteady-state heat-transfer coefficients derived from the integral form of the energy-conservation law. Approximation functions are used to represent the unsteady temperature field, which permits processing of the test data.

Analysis

The calculation method is valid for a one-dimensional heat flow in addition to rotational and spherical symmetry. Temperature-dependent material properties are taken into account, and the unsteady fluid temperature $T_\delta=T_\delta(t)$ also is considered. The number of measurement locations is assumed to be $z>1$. The unsteady temperature field $T=T(x,t)$ is presented in the form of $n'+1$ test triplets (T_n,x_n,t_n) in which the summation index $n=0,1,2,\ldots n'$. It is assumed that T_n is represented by the approximating polynomial

$$T=\sum_{(i)}\sum_{(j)} a_{ij}\,x^i t^j \tag{1}$$

where $i=0,1,2,\ldots,i'$ and $j=0,1,2,\ldots,j'$. The terms i' and j' of the polynomial may be chosen at will. The definition of the polynomial is restricted to an area in the x and t plane encompassing the experimental measurement locations, in which the distances between these points need not be equal. In principle, min. $\{x_n\}$ has to be placed near the wall surface where $x=x_0$, thus avoiding inadmissibly large extrapolations

Presented as Paper 76-106 at the AIAA 14th Aerospace Sciences Meeting, Jan. 26-28, 1976, Washington, D.C.; submitted July 8, 1976; revision received Oct. 6, 1976.

Index categories: Heat Conduction; Nozzle and Channel Flow; Liquid Rocket Engines.

*Scientist, Institute for Chemical Propulsion and Engineering of the German Aerospace Research Establishment.

in the calculation of the wall surface temperature

$$T_w = \sum_{(i)} \sum_{(j)} a_{ij}\, x_0^i\, t^j \tag{2}$$

To determine the coefficient matrix (a_{ij}) of the polynomial, the Gaussian least squares method may be used, resulting in a minimum of the sum

$$Q = \sum_{(n)} [\,(\sum_{(i)} \sum_{(j)} a_{ij} x_n^i\, t_n^j - T_n)^2\,] \stackrel{!}{=} \min \tag{3}$$

Q also can be conceived as a function of $(i'+1)$ $(j'+1)$ variables of a_{ij}. Then the conditions for min. $\{Q\}$ are

$$\left(\frac{\partial Q}{\partial a_{ij}}\right)_{i=\bar{i},j=\bar{j}} = 0$$
$$(\bar{i}=0,1,2,\ldots,i';\ \bar{j}=0,1,2,\ldots,j') \tag{4}$$

where $\bar{i}$ and $\bar{j}$ are introduced to discriminate the summation indices. Differentiation results in the linear inhomogeneous system

$$\sum_{(n)} [x_n^{\bar{i}}\, t_n^{\bar{j}} \sum_{(i)} \sum_{(j)} a_{ij} x_n^i\, t_n^j] - \sum_{(n)} x_n^{\bar{i}}\, t_n^{\bar{j}}\, T_n = 0$$
$$(\bar{i}=0,1,2,\ldots,i';\ \bar{j}=0,1,2,\ldots,j') \tag{5}$$

which features a symmetric coefficient matrix in its main diagonal. The limited Gaussian algorithm[9] offers a solution, thus determining a coefficient matrix (a_{ij}) for the polynomial terms i' and j' that were chosen. If these terms are

$$i' = 1,2,\ldots,i'_{\max} \tag{6a}$$

$$j' = 1,2,\ldots,j'_{\max} \tag{6b}$$

the matrices derived from the $i'_{\max} \cdot j'_{\max}$ cases, according to Eq. (5), permit the isolation of a matrix (a_{ij}) which features the smallest sum min. $\{Q\}$. But there are other selection criteria. By using all pairs of values (x_n, t_n), an approximation polynomial which results in the least deviations from zero when introduced into Fourier's differential equation can be found. But, in any case, the set of experimental data is replaced by Eq. (1) as an analytical function. For example, if temperature T_δ is not available as a constant or as an analytical function $T_\delta = T_\delta(t)$ but as a pair of measured quantities these values have to be substituted by an approximation polynomial

$$T_\delta = \sum_{(k)} a_k\, t^k \tag{7}$$

where $k = 0,1,2,\ldots,k'$. For an isotropic heat conductor, the material functions $\lambda = \lambda(T)$ and $K = K(T)$ generally are known. From this, the approximation polynomials

$$\lambda = \sum_{(\mu)} b_\mu\, T^\mu \tag{8}$$

$$\frac{\lambda}{K} = \sum_{(\nu)} c_\nu\, T^\nu \tag{9}$$

can be derived, where $\mu = 0,1,2,\ldots,\mu'$ and $\nu = 0,1,2,\ldots,\nu'$. For the selected polynomial degrees k', μ', and ν', Gauss' normal equations provide the coefficients (a_k), (b_μ), and (c_ν). When Eqs. (1,2,7, and 8) are introduced into the heat-transfer condition

$$\alpha(T_\delta - T_w) = -\left[\lambda \frac{\partial T}{\partial x}\right]_{x=x_0} \tag{10}$$

differentiation will supply the required heat-transfer coefficient

$$\alpha = -\sum_{(i)} \sum_{(j)} (a_{ij}\, i x_0^{i-1} t^j) \cdot \frac{\sum_{(\mu)} [b_\mu (\sum_{(i)} \sum_{(j)} a_{ij} x_0^i t^j)^\mu]}{\sum_{(k)} a_k t^k - \sum_{(i)} \sum_{(j)} a_{ij} x_0^i\, t^j} \tag{11}$$

In some cases this relation may be a rather rough approximation because approximation polynomials show an increasing deviation near their limits of definition. This deviation mainly affects the temperature gradient $\partial T/\partial x$ at $x = x_0$ of Eq. (10). For this reason, the integral form of the energy-conservation law will be used to calculate $\alpha = \alpha(t)$.

The heat balance can be established for a control volume (Fig. 1) that is represented by a straight prism of height $(x_1 - x_0)$ in the one-dimensional model and by a sector of a hollow cylinder or a hollow sphere with the radii x_0 and x_1 in the cases of rotational or spherical symmetry. The difference of the heat flow entering at x_0 and emerging at x_1 must equal the change of stored energy. In the x direction, the boundaries of the control volume are $x_1 \le \max\{x_n\}$ and x_0, where $x_0 < x_1$. The wall surface at $x = x_0$ is A_0. In a one-dimensional temperature field $\epsilon = 0$; in a field of rotational symmetry $\epsilon = 1$; and in a spherical-symmetry field $\epsilon = 2$. Then, the heat balance equation is

$$A_0 \alpha (T_\delta - T_w) - A_0 \left(\frac{x_1}{x_0}\right)^\epsilon \left[-\lambda \frac{\partial T}{\partial x}\right]_{x=x_1} = \frac{\mathrm{d}}{\mathrm{d}t} \int_{x_0}^{x_1} A_0 \left(\frac{x}{x_0}\right)^\epsilon \rho c T\, x^\epsilon\, \mathrm{d}x \tag{12}$$

From this, the heat-transfer coefficient

$$\alpha(t) = \frac{A - B}{C}$$

$$\min.\ \{t_n\} \le t \le \max.\ \{t_n\} \tag{13}$$

is obtained by using the abbreviated terms

$$A = \frac{\mathrm{d}}{\mathrm{d}t} \int_{x_0}^{x_1} \zeta c T\, x^\epsilon\, \mathrm{d}x \tag{14}$$

$$B = x_1^\epsilon \left[\lambda \frac{\partial T}{\partial x}\right]_{x=x_1} \tag{15}$$

$$C = x_0^\epsilon\, (T_\delta - T_w) \tag{16}$$

Equation (12) also provides the heat flux at $x = x_0$

$$q(t) = (A - B)/x_0^\epsilon \tag{17}$$

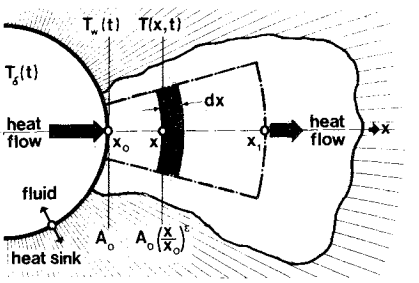

Fig. 1 Energy balance for the control volume

The attempt to obtain α or q not from Eq. (12) but from an exact solution of Fourier's differential equation

$$\rho c\frac{\partial T}{\partial t}=\frac{\partial}{\partial x}\left(\lambda\frac{\partial T}{\partial x}\right)+\lambda\frac{\epsilon}{x}\frac{\partial T}{\partial x} \tag{18}$$

appears to be unpromising. Equations (14) and (9), as well as $\lambda/K=\rho c$, provide

$$A=\int_{x_0}^{x_1}\left\{x^{\epsilon}\sum_{(\nu)}\left[c_{\nu}(\nu+1)T^{\nu}\frac{\partial T}{\partial t}\right]\right\}dx \tag{19}$$

and, introducing Eq. (1) results in

$$A=\int_{x_0}^{x_1}\left\{\left(x^{\epsilon}\sum_{(i)}\sum_{(j)}a_{ij}x^{i}jt^{j-1}\right)\cdot\sum_{(\nu)}\left[c_{\nu}(\nu+1)\left(\sum_{(i)}\sum_{(j)}a_{ij}x^{i}t^{j}\right)^{\nu}\right]\right\}dx \tag{20}$$

For polynomial degrees $\nu'>1$, there is only a numerical solution to this integral which can be obtained by dividing the interval (x_0,x_1) into $(m'+1)$ partial intervals

$$\Delta x=(x_1-x_0)/(m'+1) \tag{21}$$

If the summation index $m=0,1,2,\ldots,m'$ and

$$x_m=x_0+m\,\Delta x \tag{22}$$

then Eq. (20) is transformed to

$$A=\Delta x\sum_{(m)}\left\{\left(x_m^{\epsilon}\sum_{(i)}\sum_{(j)}a_{ij}x_m^{i}jt^{j-1}\right)\cdot\sum_{(\nu)}\left[c_{\nu}(\nu+1)\left(\sum_{(i)}\sum_{(j)}a_{ij}x_m^{i}t^{j}\right)^{\nu}\right]\right\} \tag{23}$$

Using Eqs. (1, 2, 7, and 8), Eqs. (15) and (16) become

$$B=x_1^{\epsilon}\sum_{(\mu)}\left[b_{\mu}\left(\sum_{(i)}\sum_{(j)}a_{ij}x_1^{i}t^{j}\right)^{\mu}\right]\sum_{(i)}\sum_{(j)}a_{ij}ix_1^{i-1}t^{j} \tag{24}$$

$$C=x_0^{\epsilon}\left(\sum_{(k)}a_k t^{k}-\sum_{(i)}\sum_{(j)}a_{ij}x_0^{i}t^{j}\right) \tag{25}$$

Equations (13 and 23-25) permit the calculation of $\alpha=\alpha(t)$ without imposing limitations on polynomial degrees μ' and ν'.

In many cases, it may suffice to use constant material properties $\lambda=\bar{\lambda}$ and $K=\bar{K}$ which allow an analytical solution to the integral of Eq. (20). Equations (23-25) then are replaced by

$$A=\frac{\bar{\lambda}}{\bar{K}}\sum_{(i)}\sum_{(j)}a_{ij}\left(x_1^{i+\epsilon+1}-x_0^{i+\epsilon+1}\right)jt^{j-1}(i+\epsilon+1)^{-1} \tag{26}$$

$$B=x_1^{\epsilon}\bar{\lambda}\sum_{(i)}\sum_{(j)}a_{ij}i\,x_1^{i-1}t^{j} \tag{27}$$

$$C=x_0^{\epsilon}\left(T_{\delta}-\sum_{(i)}\sum_{(j)}a_{ij}\,x_0^{i}\,t^{j}\right) \tag{28}$$

Because there are no limitations to be imposed on the tests, all of these equations offer some advantages in determining α as compared with a solution of Fourier's linear differential equation.

The functions $\alpha=\alpha(t)$, $T_{\delta}=T_{\delta}(t)$, and $T_w=T_w(t)$ being known, time t, for example, may be eliminated by $\alpha=\alpha(T_{\delta}/T_w)$. This can be done by forming pairs of values $(\alpha,T_{\delta}/T_w)$ for different times within the defined limits of Eq. (1) and representing these by an approximation polynomial

$$\alpha=\sum_{(\sigma)}d_{\sigma}\left(\frac{T_{\delta}}{T_w}\right)^{\sigma} \tag{29}$$

where $\sigma=0,1,2,\ldots,\sigma'$.

In addition the derived relations are also valid when $x_0>x_1$ (outside heating) and $x_1\geq\min.\{x_n\}$. The heat flow then changes its sign because its direction is reversed and now opposed to the positive x direction.

It is convenient to reduce the number of coefficients of the approximation function $T(x,t)$ and to simplify data processing by using power functions. One of these approximation functions of sufficient precision is

$$T=a\,x^{b}\,t^{d} \tag{30}$$

where $x>0$ and $t>0$. The system of equations used to determine the coefficient a and exponents b and d is linear if the Gaussian demand of least squares is stated as follows

$$Q=\sum_{(n)}[\ln(a\,x_n^{b}t^{d})-\ln T_n]^2\overset{!}{=}\min \tag{31}$$

Then the conditions for a minimum of sum Q are

$$\partial Q/\partial\omega=0;\qquad \omega=a,b,d \tag{32}$$

Strictly speaking, the origin of the x coordinate can be chosen freely in the case of one-dimensional heat flow ($\epsilon=0$). Since Q is a function of this origin, the additional condition $\partial Q/\partial x_0=0$ should be observed when $Q_{\min}$ is determined. The wall surface temperature at $x=x_0$ results from Eq. (30)

$$T_w=a\cdot x_0^{b}\cdot t^{d} \tag{33}$$

It is useful to fit material properties by power functions in T. For thermal conductivity $\lambda=\lambda(T)$ and the product $\rho c=\lambda/K$, the material-property functions are

$$\lambda=F\cdot T^{G} \tag{34}$$

$$\lambda/K=D\cdot T^{E} \tag{35}$$

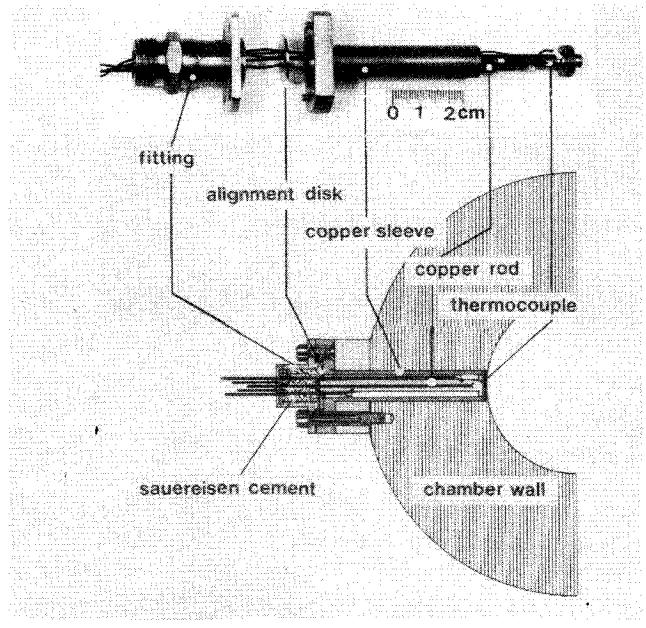

Fig. 2 Heat-flux probe.

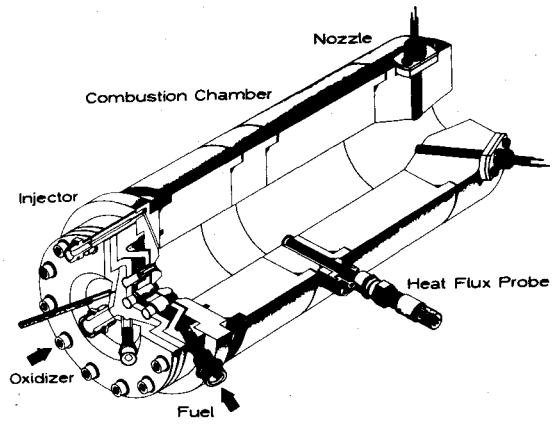

Fig. 3 Experimental rocket engine for high-energy propellant combinations.

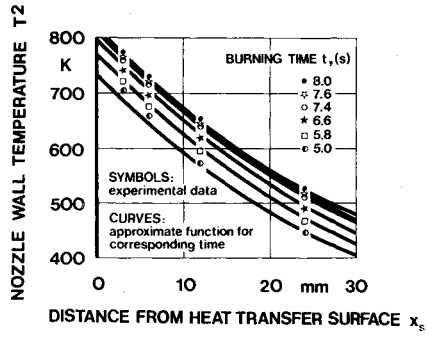

Fig. 4 Nozzle-wall temperature distribution approximated by a polynomial.

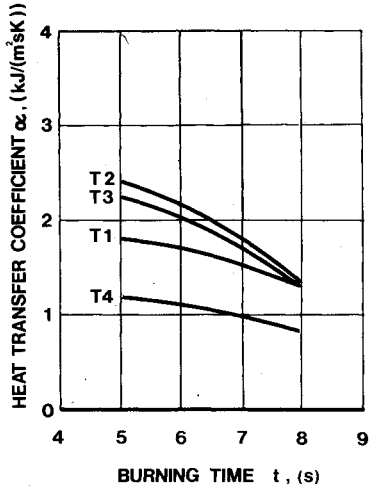

Fig. 5 Local hot-gas-side heat-transfer coefficients as a function of burning time.

Here F and D, as well as G and E, are material characteristics. When the approximation function of Eq. (30), the wall surface temperature of Eq. (33), and the material-property functions of Eqs. (34) and (35) are introduced into Eqs. (14-16), the resulting equations are

$$A = D \cdot a^{E+1} d(E+1) \cdot t^{d(E+1)-1} \cdot \frac{x_1^{\,b(E+1)+\epsilon+1} - x_0^{\,b(E+1)+\epsilon+1}}{b(E+1)+\epsilon+1} \tag{36}$$

$$B = x_1^{\,\epsilon+b(G+1)-1} \cdot F \cdot b \cdot a^{G+1} \cdot t^{d(G+1)} \tag{37}$$

$$C = x_0^{\epsilon} \cdot (T_\delta - a\, x_0^b t^d) \tag{38}$$

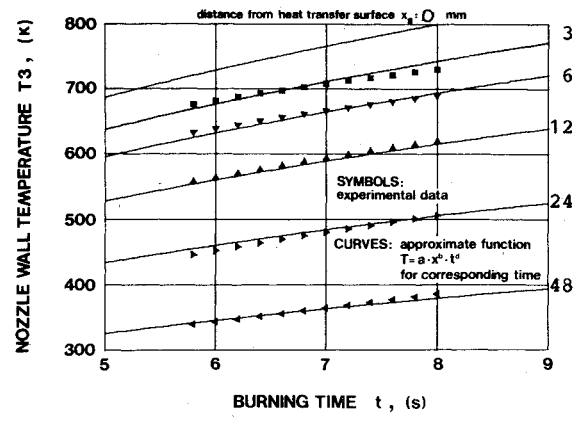

Fig. 6 Nozzle-throat wall-temperature distribution approximated by a power function.

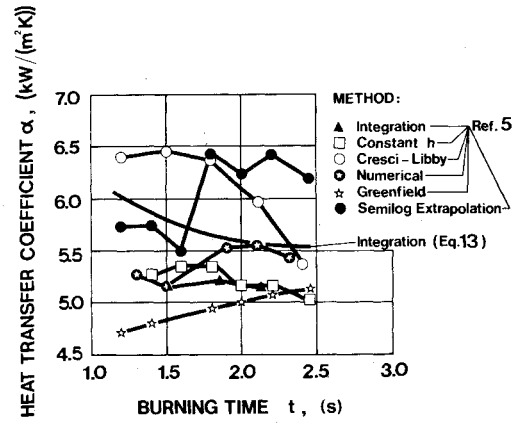

Fig. 7 Comparison of several calculation methods for the local heat-transfer coefficient[5] with the integration method, using Eq. (13).

Unlike the use of a polynomial, this permits an analytical solution to the integral across the control volume even when temperature-dependent material properties are considered.

Experimental Results

Figure 2 shows the detail of the heat-flux probe used to measure heat flux. High-conductivity copper rods 62 mm in length and 5 mm in diameter are instrumented with five chromel-alumel thermocouples. The thermocouple balls are peened into small holes drilled into the rod surface. The thermocouples are attached at distances of 3,6,12,24, and 48 mm from the heat-transferring surface. A copper sleeve is positioned around the copper rod, and soldered to the rod at its right end. The 1-mm gap between the rod and sleeve prevents heat conduction from the neighboring wall to the rod, so that the assumption of one-dimensional heat flow along the rod is justified. To avoid pulling the thermocouple wires from their position, they are set in place in the fitting with sauereisen cement. The assembled heat-flux probes then are inserted into the cavities in the nozzle and combustion chamber wall and sealed with O-rings. The interior contours of the combustion-chamber and nozzle wall then are machined to the desired dimensions, leaving their inner surfaces completely smooth.

A heavy-walled copper heat-sink thrust chamber shown schematically in Fig. 3 was used. The conical expansion nozzle consists of a single segment, but in order to provide a variable characteristic combustion-chamber length, the combustion-chamber is composed of several segments of different lengths. One heat-flux probe (T1) is installed in the combustion-chamber wall and three others (T2, T3, and T4) in the nozzle

wall at area ratios $A/A_t = 1.39$ (converging section), $A/A_t = 1$ (nozzle throat), and $A/A_t = 1.39$ (diverging section). The combustion chamber diameter is 66 mm, and the nozzle-throat diameter is 38.2 mm, giving a contraction ratio $A_c/A_t = 3$. The half-angle of the nozzle's convergent cone section is 30°, and the divergent cone half-angle is 15°. The combustion chamber has a characteristic length L^* of 0.46 m. The experimental rocket engine produces from 30 to 150 daN of thrust, depending on the combustion chamber pressure and mixture ratio.

Testing of an experimental rocket engine having a nine-element triplet injector and using the propellant combination fluorine/hydrogen serves as an example for the applicability of the procedure reported herein. The operational parameters of the engine are combustion chamber pressure $p_c = 5.8$ bar, mixture ratio $\dot{m}_O/\dot{m}_F = 11.0$, combustion temperature $T_\delta = 3860$ K, characteristic velocity efficiency $\eta_c{}^* = 0.98$, and total burning time $t_{tot} = 8.4$ sec. Figure 4 shows the measured temperature field $T(x,t)$ in the convergent-nozzle heat-flux probe T2, as well as the approximation polynomials resulting from Eq. (1). Here x_s (where $x_s = x - x_0$) stands for the distance of the measurement location from the heat-transfer surface. The average error of this approximation function can be regarded as sufficiently small. The hot-gas-side heat-transfer coefficient $\alpha = \alpha(t)$ determined according to Eq. (13), is shown in Fig. 5 for all four heat-flux probes (T1-T4). The temperature dependence of the material properties is taken into account according to Eqs. (8 and 9). Figure 6 presents the measured temperature field $T = T(x,t)$, in conjunction with the power function used according to Eq. (30) for the heat-flux probe in the nozzle throat. From this, it is evident that the measured temperature field is approximated sufficiently by the power function. In this example, the average relative error amounts to 0.737%, which leads to an error of about 5% for the calculated heat flux. Concerning the use of power functions, some critical remarks have to be made. In the general case of unsteady heat flow, the heat flux, as well as the heat-transfer coefficient, may increase or decrease as a function of time. If power functions are used to approximate the temperature field, the partial derivative $\partial T/\partial x$ always increases with time so that in many cases the heat-transfer coefficient cannot be determined by means of Eq. (10).

Figure 7 shows a comparison between the method presented in this paper and the procedures described in Ref. 5, in which a 2400-lb-thrust oxygen/ammonia rocket engine was used. The approximation was made by means of a power function and temperature-dependent material properties according to Eqs. (30, 34, and 35). Unlike other current procedures, the method presented in this paper provides a continuous function for the heat-transfer coefficient in relation to time or, if desired, to wall surface temperature T_w.

References

[1]Pulkert, G., "Entwicklung eines Raketentriebwerkes mit 5 kN Vakummschub für Flüssig-Wasserstoff/Flüssig-Fluor," *Raumfahrtforschung*, Vol. 16, July 1962, pp. 180-187.

[2]Quentmeyer, R. J., Schacht, R. L., and Jones, W. L., "Hot-Gas-Side Heat Transfer With and Without Film Cooling on a Simulated Nuclear Rocket Chamber Using H_2-O_2," NASA TN D-6638, 1972.

[3]Schacht, R. L. and Quentmeyer, R. J., "Axial and Circumferential Variations of Hot-Gas-Side Heat Transfer Rates in a Hydrogen-Oxygen Rocket," NASA TN D-6396, 1971.

[4]Schacht, R. L., Quentmeyer, R. J., and Jones, W. L., "Experimental Investigations of Hot-Gas-Side Heat-Transfer Rates for a Hydrogen-Oxygen Rocket," NASA TN D-2832, 1965.

[5]Liebert, C. H., Hatch, J. E., and Grant, R. W., "Application of Various Techniques for Determining Local Heat-Transfer Coefficients in a Rocket Engine," NASA TN D-277, 1960.

[6]Carslaw, H. S. and Jaeger, J. C., *Conduction of Heat in Solids*, Oxford University Press, London, 1959.

[7]Cresci, R. J. and Libby, P. A., "Some Heat Conduction Solutions Involved in Transient Heat-Transfer Measurements," TN 57-236, 1957, Wright Air Development Center.

[8]Howard, F. G., "Single-Thermocouple Method for Determining Heat Flux to a Thermally Thick Wall," NASA TN D-4737, 1968.

[9]Zurmühl, R., *Praktische Mathematik*, Springer Verlag, Berlin, 1965.